

# Development of Power Robot Hand with Shape Adaptability Using Hydraulic McKibben Muscles

Mayuko Mori, Koichi Suzumori, *Member, IEEE*, Shuichi Wakimoto, Takefumi Kanda, *Member, IEEE*, Masayuki Takahashi, Takashi Hosoya, Emi Takematu

**Abstract**— We have developed a hydraulic McKibben artificial muscle which realizes great force density approximately ten times larger than the other conventional actuators. In this paper, we have applied this muscle to a power robot hand. The hand finger consists of metal links and the muscles. The contraction of the muscles generates the bending motion of the fingers. This hand has large holding capacity and shape adaptability to grasp objects. The experiments show that maximum holding force of the hand is 5000N. It can hold three types of different shaped objects; cylindrical objects of  $\phi$  267mm and  $\phi$  165mm in diameter and a square cross section of width 200mm in side. This hand can be applied to various applications, for example rescue robots in disaster area and forestry industry.

## I. INTRODUCTION

In fields such as disaster recovery, forestry and construction, it would be useful to have small lightweight actuators that can exert a large force. There is consequently a strong demand for the implementation of small lightweight robots and tools in these fields. Fig. 1 shows the typical force exertion and displacement characteristics of four types of actuator that are currently in general use.

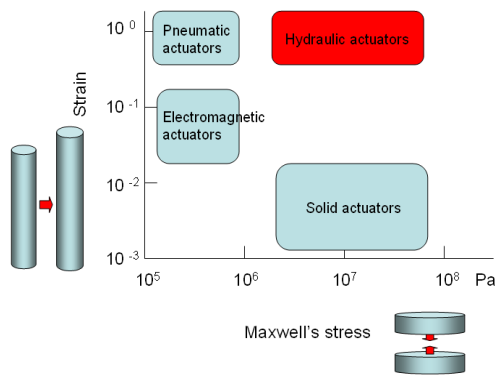


Fig. 1: Maxwell's stress and strain of four typical actuators[1]

Here, the horizontal axis shows the exerted force per unit area (Maxwell's stress) at the sites where forces are generated in each actuator as an indication of the exerted force, and the vertical axis shows the ratio of the maximum working stroke

length to the size of the actuator as an indication of the amount of displacement[1]. As this figure shows, hydraulic actuators exert large forces and have large displacements. The authors have developed a high-pressure hydraulic artificial muscle that is suitable for use in McKibben artificial muscles and has particularly large force-to-volume and force-to-mass ratios[2]-[5]. To allow it to operate at high working pressures, we replaced the conventional pneumatic drive with a high-pressure water hydraulic system, and we used high-strength PBO (p-phenylene-2, 6-benzobisoxazole) fibers to fabricate the sleeve[6]. We also developed a new end shape and fixing method for artificial muscles to enable them to withstand high pressures. When fabricating the sleeve, we considered the relationship between the external diameter of the rubber tube and the fiber weave angle and the number of fiber bundles constituting the sleeve, and we designed a sleeve of a suitable size that is capable of a large amount of contraction and is able to uniformly protect the rubber tube. Furthermore, to prevent bending of the sleeve fibers and disruption of the weave angle from occurring as a result of repeated contractions, we fabricated and used a three-layer rubber tube consisting of the sleeve sandwiched between two rubber layers. With this three-layer structure, it was possible to prevent the strength of the PBO fibers from being reduced by ultraviolet light. By subjecting this artificial muscle to contraction force measurement tests, we confirmed that it is capable of a contraction force of 28 kN when supplied with a maximum pressure of 4 MPa[5].

In this paper, based on the achievements of these studies, we discuss the development of a new artificial muscle for robot hands that can lift heavy objects, and a power hand capable of copying the gripping of objects with various shapes by varying flexibility of the artificial muscle. Although studies have already been made of robots that use flexible actuators to adapt to the shape of objects they are handling[7]-[9] and robots for heavy lifting[10]-[12], none of them have combined the ability to adapt to the shape of objects with the ability to exert large forces. The hand we developed has both of these characteristics, and it is thus expected that it will be useful for applications such as forestry and disaster rescue where it is not possible to determine the shape of objects that need to be gripped.

Manuscript received September 14, 2009. This work was supported by Japan Science and Technology agency as a "Collaborative Development of Innovative Seeds" project.

## II. DEVELOPMENT OF A WATER HYDRAULIC MCKIBBEN ARTIFICIAL MUSCLE

McKibben artificial muscles were developed by Schulte et al. in the 1950s[13]. Hitherto they have been driven with compressed air, but in this study to make it possible to apply high pressures, we employed water hydraulic drive and we used high-strength PBO sleeve fibers[6]. To make it capable of withstanding high-pressure water hydraulic actuation, we used the method shown below where the sleeve is folded back and secured together with a swaged end connector. An overview of this artificial muscle is shown in Fig.2.



Fig. 2: Overview of the artificial muscle

In a McKibben artificial muscle that operates at high pressure, the application of water hydraulic pressure to the sleeve causes a large load to act along the axis of the actuator, and this can occasionally cause problems such as friction at fixed parts and breakage of sleeve fibers due to insufficient strength of the fibers themselves[5]. To address these problems, the authors have hitherto experimented with a method where the sleeve is fixed by passing it through a sleeve fixing ring and folding it back, and a method that uses the same sort of plugged fixture as a high-pressure oil hydraulic hose. We designed our new artificial muscle using the latter method since it is more lightweight and durable. Fig.3 shows a cross-sectional view of this structure.

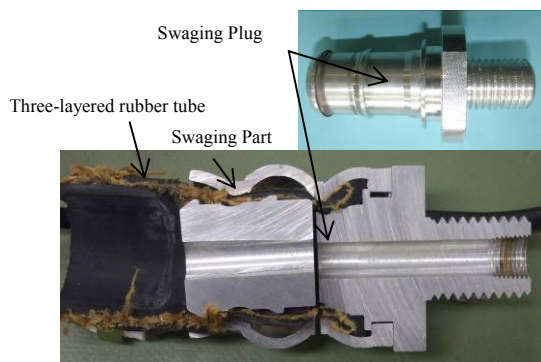


Fig. 3: Example of plugging at the end of the muscle

We made the sleeve from high-strength PBO fibers. PBO fibers have excellent heat resistance and fire resistance, and can withstand a high tensile stress of 5.8 GPa[6]. For this study, we constructed a sleeve from 96 threads at a weave angle of 25° using twisted multi-filament fiber bundles with a thickness of 6600 [T(desi-tex)]. By twisting the fiber bundles, it is easy to configure a sleeve from PBO fibers that easily become frayed if left as single fibers.

We used natural rubber as the rubber material, and to prevent the strength of the PBO fibers from reducing due to fraying of the sleeve, disruption of the weave angle and exposure to ultraviolet light, we employed a three-layer structure with the sleeve sandwiched between two layers of rubber. The cross-sectional structure of the three-layer rubber tube is shown in Fig. 4.

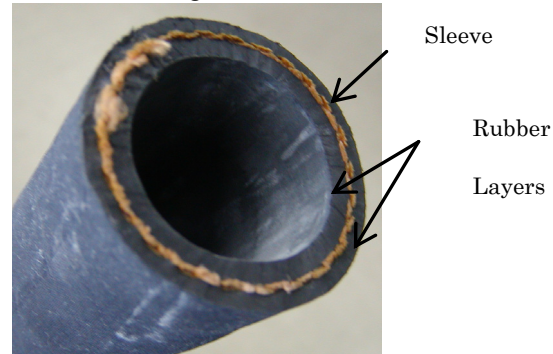


Fig.4: Cross section of the three layers rubber tube

To fabricate this three-layer rubber tube, we wove the PBO fiber sleeve on the un-vulcanized inner rubber tube layer, then applied the outer rubber tube layer and vulcanized the resulting structure. In this way, we were able to bond together the inner rubber layer, PBO fiber sleeve and outer layer rubber.

This artificial muscle has an internal diameter of 30 mm, an external diameter of 40 mm, and a total length of 600 mm excluding the fixing screw parts. An M24 screw thread formed at the end is used to fix the muscle to a hand link (described below). In tests, this artificial muscle was able to exert a contracting force of up to 28 kN when subjected to a pressure of 4 MPa. The muscle was pressurized by a high-pressure pump. Fig. 5 shows the relationship between the contracting force and contraction ratio of this muscle. As this figure shows, the measured values were more or less the same as the design values[14].

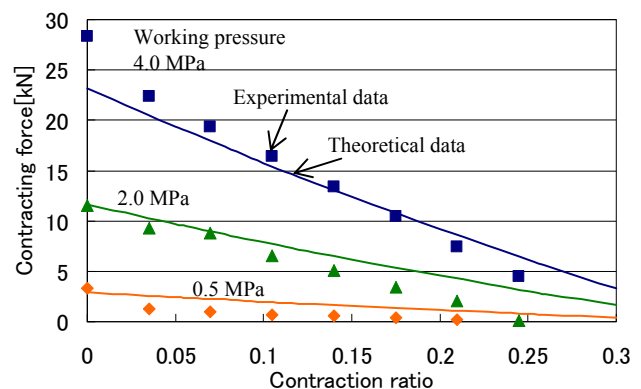


Fig. 5: Contracting force and contraction ratio of the artificial muscle[14]

We compared this artificial muscle with four typical actuators that are currently in widespread uses for high force mechanisms— an oil hydraulic cylinder, a pneumatic cylinder, a ball screw and a conventional pneumatic

McKibben artificial muscle. These were evaluated using four parameters — the force density volume (FDV) and force density mass (FDM), which express the generated force divided by the volume and mass of the actuator respectively, and the energy density volume (EDV) and energy density mass (EDM), which are the volume ratio and mass ratio obtained by dividing the maximum value of the energy generated in a single stroke action by the volume and mass of the actuator respectively. EDV and EDM are new actuator evaluation parameters defined by Kuribayashi et al[15]. Especially, EDVs and EDMs are useful for non-linear actuators which the generating forces depend on their displacements. Using the parameters  $f$ ,  $x$ ,  $m$  and  $v$  to represent the actuator's generated force, displacement, mass and volume, these four parameters can be expressed as shown by Equations (1) through (4) below.

$$FDV = \frac{f}{v} \quad (1)$$

$$FDM = \frac{f}{m} \quad (2)$$

$$EDV = \frac{1}{v} \int f dx \quad (3)$$

$$EDM = \frac{1}{m} \int f dx \quad (4)$$

The FDV and FDM of our new artificial muscle were  $3.71 \times 10^{-2} \text{ N/mm}^3$  and  $1.17 \times 10^4 \text{ N/kg}$  respectively, and its EDV and EDM were  $3.03 \text{ J/mm}^3$  and  $9.2 \times 10^5 \text{ J/kg}$  respectively. All these values were between 2 and 98 times higher than the values obtained with conventional actuators. Table 1 shows the specifications of high contracting force artificial muscles and four typical conventional actuators which are almost in same size with the developed muscles, together with the values of each of the four parameters mentioned above. Working pressures of the fluid actuators shown in Table 1 are based on practical values currently used. Cross sections shown in Table 1 mean the outer size of the

actuators.

### III. DESIGN OF HAND MECHANIS

To construct the fingers of the hand, we combined our artificial muscle with duralumin links, steel shafts, and stainless steel plates. The hand links were made to undergo contraction movements by mounting artificial muscles inside them, resulting in a bending action as shown in Fig. 6.

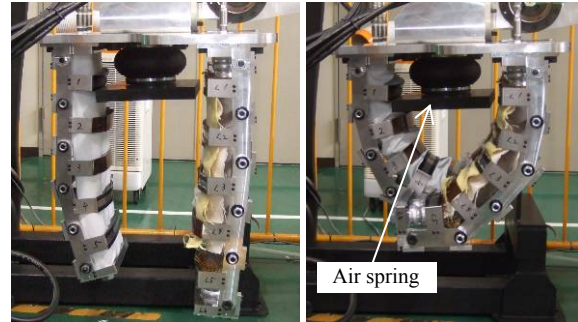


Fig. 6: Bending motion of the power robot hand (2)

Fig. 7 shows a hand we produced consisting of three fingers fixed to a plate. Two of these fingers were fitted with two artificial muscles, and the other one was fitted with three artificial muscles. An air spring was attached in the palm of the hand in order to hold gripped objects in place.

Figure 8 shows the detailed structure of a single finger. It has 5 links connected by shafts with a spacing of 140 mm between links. The narrow fingers are 193 mm wide, and the wide fingers are 263mm wide.

Assuming the fingers of the hand bend into circular arcs, we derived the relationship between the contraction of the artificial muscle and the amount of curvature of the fingers. The gripping operation of the robot hand is illustrated schematically in Fig. 9.

Table 1 Comparison of developed muscle and typical conventional linear actuators. Based on the literatures[16]-[19].

|                               | Hydraulic cylinder[16] | Air cylinder[17]     | Ball screw and motor[18] | Air artificial muscle[19] | Developed muscle      |
|-------------------------------|------------------------|----------------------|--------------------------|---------------------------|-----------------------|
| Mass* kg                      | 2.79                   | 1.36                 | 5.1                      | 0.29                      | 2.4                   |
| Displacement mm               | 550                    | 574.0                | 400                      | 175                       | 110                   |
| Maximum exerting force N      | 439.6                  | 343                  | 684                      | 1650                      | 28000                 |
| Volume* mm <sup>3</sup>       | $4.94 \times 10^5$     | $5.28 \times 10^5$   | $1.698 \times 10^6$      | $6.73 \times 10^5$        | $7.54 \times 10^5$    |
| Length mm                     | 700                    | 700                  | 662                      | 700                       | 600                   |
| Cross section mm <sup>2</sup> | 706.5                  | 754.4                | 2565                     | 961.6                     | 1256                  |
| FDV * N/mm <sup>3</sup>       | $8.9 \times 10^{-4}$   | $6.5 \times 10^{-4}$ | $3.8 \times 10^{-4}$     | $2.45 \times 10^{-3}$     | $3.71 \times 10^{-2}$ |
| FDM * N/kg                    | $1.6 \times 10^2$      | $2.5 \times 10^2$    | $1.3 \times 10^2$        | $2.9 \times 10^2$         | $1.17 \times 10^4$    |
| EDV * J/mm <sup>3</sup>       | 0.49                   | 0.37                 | 0.16                     | 0.19                      | 3.03                  |
| EDM * J/kg                    | $8.67 \times 10^4$     | $1.45 \times 10^5$   | $5.36 \times 10^4$       | $4.53 \times 10^5$        | $9.2 \times 10^5$     |
| Working pressure MPa          | 14                     | 0.7                  | -                        | 0.7                       | 4                     |

\* The power sources are not included.

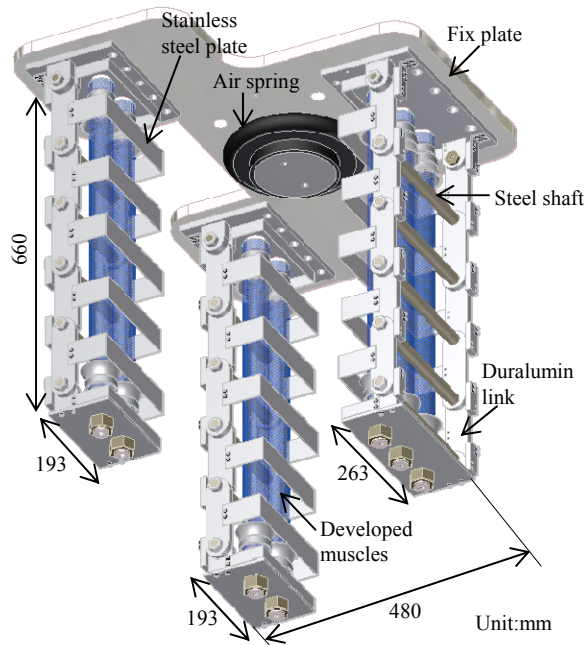


Fig. 7: Overview of the power robot hand

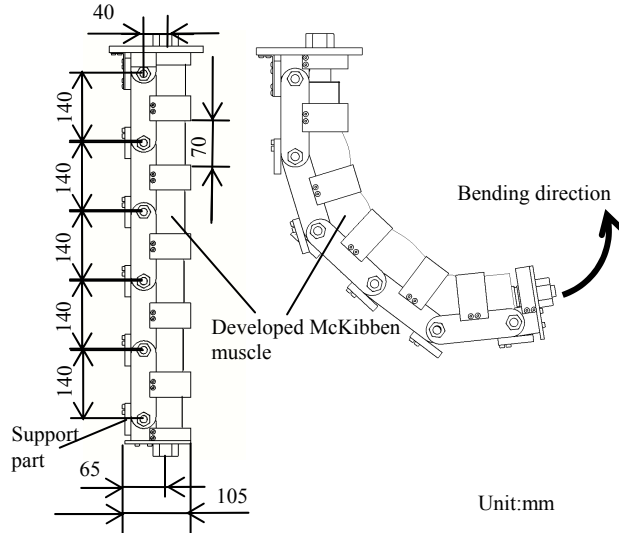


Fig. 8: Finger structure

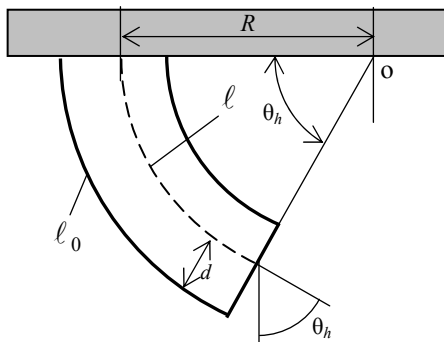


Fig. 9: Geometrical model of power hand bending

In this figure, the dashed line shows the locus of the artificial muscle's loading position. The parameters  $l$ ,  $l_0$ ,  $d$  and  $R$  represent the length of the artificial muscle, the total length of the links, the distance from the link position to the

artificial muscle loading position, and the bending radius of the finger.  $l_0$  assumed to be equal to the initial length of the artificial muscle. In this design,  $l_0=660\text{mm}$ ,  $d=40\text{mm}$ . If  $\theta_h$  is the bending angle at the end of the hand, then the relationships of Equations (5) and (6) hold.

$$\theta_h = \frac{l_0 - l}{d} \quad (5)$$

$$R = \frac{l}{l_0 - l} \cdot d \quad (6)$$

As these equations show, reducing the loading position  $d$  of the artificial muscle results in a larger bending angle so that the curvature of the hand becomes larger. When the hand is in the unloaded state gripping nothing,  $l$  is 550mm resulting in  $l_0 - l = 110$  mm,  $\theta_h = 157^\circ$  and  $R = 137.3$  mm. This bending angle is proper for stable holding of objects.

#### IV. DESIGN OF WATER HYDRAULIC DRIVE SYSTEM

##### A. Overview of water hydraulic drive system

We designed the water hydraulic unit so that it could open and close the fingers of the hand in less than 10 seconds and was capable of applying a maximum pressure of at least 2 MPa. Water hydraulic pumps differ from oil hydraulic pumps in that few of them operate from a low-pressure high-flow-rate region to a high-pressure low-flow-rate region. For this study we developed a water hydraulic drive system that switches between two pumps. Fig. 10 shows the circuit diagram of this water hydraulic unit, and Table 2 summarizes the specifications of the equipment used to construct the water hydraulic unit. The two pumps are connected to separate solenoid valves that open and close when the pumps are switched on and off. The pumps are also connected to non-return valves to stop water flowing backwards when pressure is applied to the hand. Drainage is performed through valve 3, and a pressure sensor detects the pressure in this water hydraulic system.

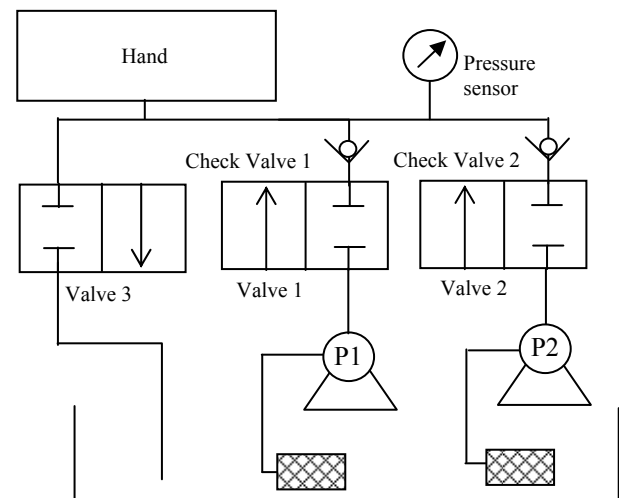


Fig. 10: The water control unit used to drive the robot hand

Table 2 Water hydraulic device specifications

|               | Pipe size | Inlet pressure | Inlet flow quantity | Pressure loss |
|---------------|-----------|----------------|---------------------|---------------|
| Valve 1       | 1-1/2     | 0.26MPa        | 450 l/min           | 1~3kPa        |
| Valve 2       | 3/8       | 3.5MPa         | 9l/min              | 1~5kPa        |
| Valve 3       | 1         | 3.5MPa         | 230 l/min           | 1~5kPa        |
| Check valve 1 | 1-1/2     | 0.26MPa        | 280 l/min           | 1kPa          |
| Check valve 2 | 3/8       | 3.5MPa         | 33 l/min            | 7.2~7.4kPa    |

Of the two pumps used in this system, one is a low-pressure high-flow-rate type (P1), and the other is a high-pressure low-flow-rate type (P2). In this way, it is possible to operate the hand quickly by applying a large flow rate when the hand has not reached the object and is still unloaded, and to apply high pressure to the hand when it comes into contact with the object and starts to apply a load. By switching between the two pumps when the maximum discharge pressure of P1 is reached, it is possible to operate the hand over a wide range of pressures. Fig. 11 shows the P-Q characteristics of our water hydraulic pressure unit[20][21].

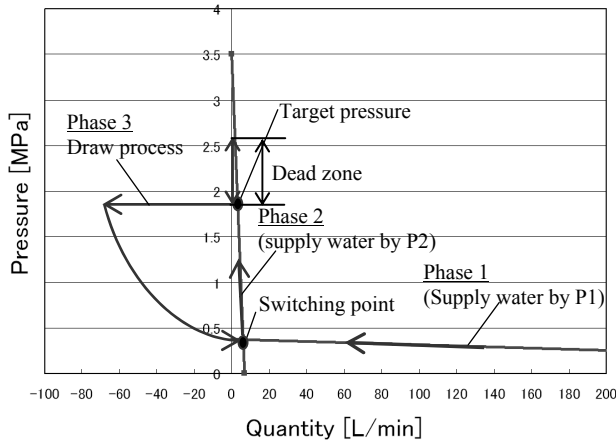


Fig. 11: P-Q curve of the pump and driving curve[20][21]

In the Phase 1 region of this figure, water is supplied to the hand by pump P1. In this region, we achieved a maximum discharge flow rate of 200 L/min. It switches over to P2 when the maximum discharge pressure of P1 has been reached, and both pumps are stopped when the target pressure has been reached. Applying a load to the hand causes the pressure inside the artificial muscles to increase, and when the deviation from the target pressure exceeds 1 MPa, the drainage valve 3 shown in Fig. 10 is opened until the pressure drops to the target value. The hand is operated by repeating these operations.

When the hand is no longer being used and the fingers are returned to their initial positions, valve 3 is opened as shown in Phase 3, and the pressure drops back to 0 MPa.

B. Control algorithm

The control equipment used to drive the water hydraulic unit is discussed here. As shown in Fig. 12, each pump and solenoid valve is controlled sequentially.

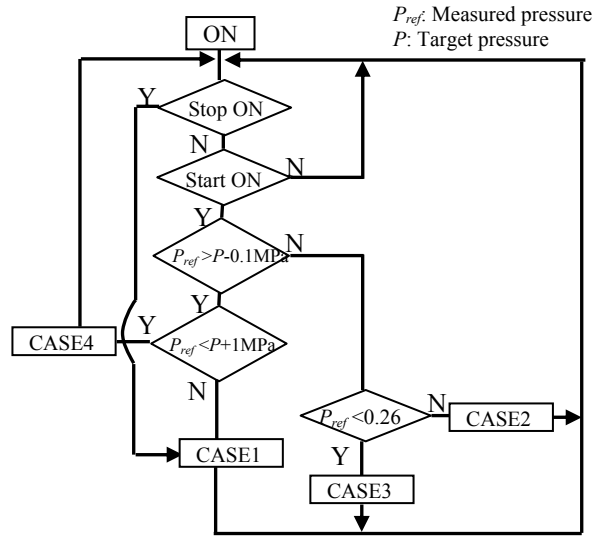


Fig. 12: Water unit control algorithm

Table 3 summarizes the state of each item of the water hydraulic unit at each of the cases shown in the Fig.12 (Case 1–4), and Fig. 13 shows the control circuit diagram.

Table 3 Working pattern of drive device

|                      | CASE1                            | CASE2                | CASE3                                | CASE4                            |
|----------------------|----------------------------------|----------------------|--------------------------------------|----------------------------------|
| P1                   | OFF                              | OFF                  | ON                                   | OFF                              |
| P2                   | OFF                              | ON                   | OFF                                  | OFF                              |
| Valve 1              | CLOSE                            | CLOSE                | OPEN                                 | CLOSE                            |
| Valve 2              | CLOSE                            | OPEN                 | CLOSE                                | CLOSE                            |
| Valve 3              | OPEN                             | CLOSE                | CLOSE                                | CLOSE                            |
| Switching conditions | STOP or $P_{ref}^* > P^* + 1MPa$ | $0.26 < P_{ref} < P$ | $P_{ref} < P$ and $P_{ref} f < 0.26$ | $P_{ref} < P - 0.1MPa < P_{ref}$ |

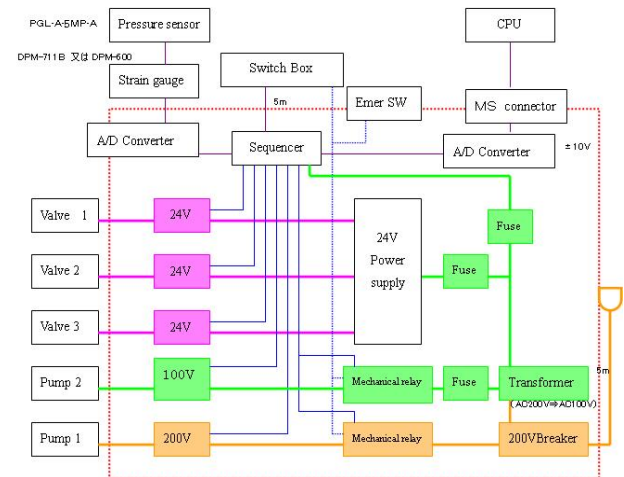


Fig. 13: Water unit control circuit

## V. EVALUATION TESTS

### A. Response speed

In hand operation tests performed using the water hydraulic drive unit discussed in section IV, we were able to grasp a cylindrical object with a diameter of 267 mm in about 9 seconds. By adjusting the hose lengths and tank positions, we were able to suppress pressure losses and increase the drive speed.

### B. Grip force measurements

#### 1) Basic evaluation

We performed basic measurements of the grip force in which the hand was made to grip a cylindrical object connected to a double-acting oil hydraulic cylinder. Loads were applied to the cylindrical object by this oil hydraulic cylinder, and the load acting on the hand (i.e., the grip force) was determined by calculation based on the pressure inside the oil hydraulic cylinder. In the basic tests, we performed experiments in two patterns where the cylindrical object was gripped horizontally and vertically, Fig. 14 shows a schematic diagram of each test system, and Fig. 15 shows an overview of the experimental apparatus.

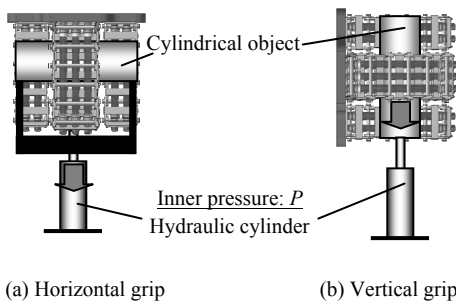


Fig. 14: The experimental setup for holding tests

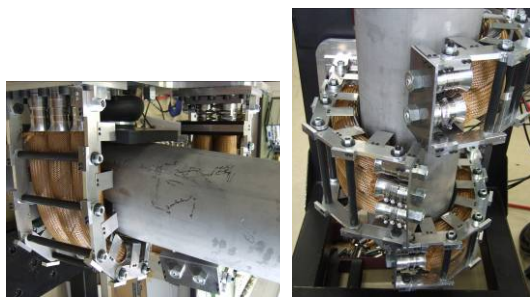


Fig. 15: The holding experiments in horizontal/vertical direction

The diameter of the object gripped by the robot hand in these tests was 267 mm. In the horizontal gripping test, a gripping force of 4000 N was exerted when an internal pressure of 1 MPa was applied to the artificial muscles, and in the vertical gripping test, a gripping force of 2000 N was exerted when an internal pressure of 1 MPa was applied. When gripping the object vertically, frictional forces between the hand and object had a large effect on the results.

At present, the link side of the hand is protected with a urethane rubber sheet. Fig.16 shows the results of these measurement tests.

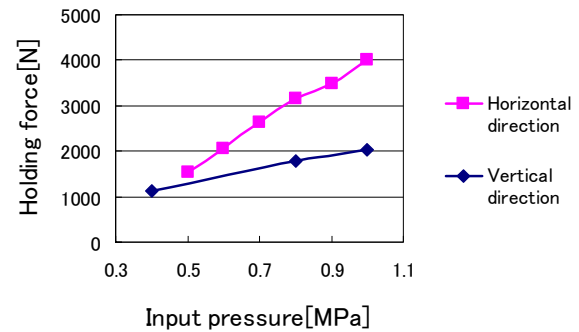


Fig. 16: Result of horizontal/vertical holding tests

#### 2) Grip test

Grip tests were performed with the robot hand mounted at the end of a robot arm and used to actually pick objects up. The experimental setup is shown in Fig. 17. These tests were performed using the three differently shaped objects shown in Fig. 18 — cylinders with diameters of 267 and 165 mm, and a rod with a square cross section of width 200 mm. The mass of these objects could be adjusted in 100 kg increments by attaching plates to the shafts at both ends of these objects. Using these objects, we performed grip tests with masses ranging from 100 to 500 kg.

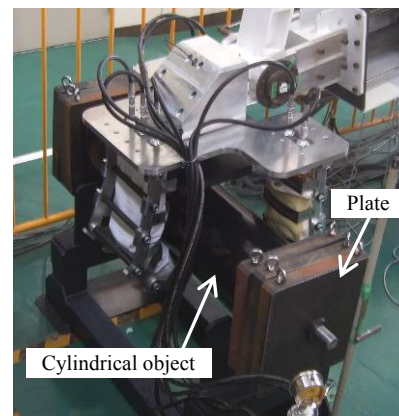


Fig. 17: Overview of the hand mounted on robot arm

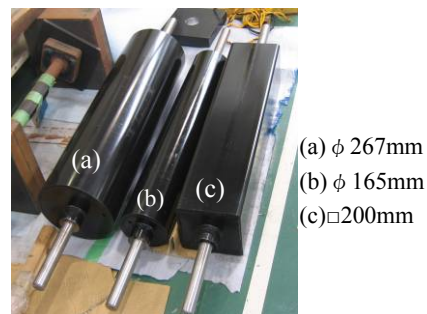


Fig. 18: Overview of the 3 types of objects for holding tests

The mass of the cylindrical object of diameter 267 mm was varied from 100 to 500 kg, and the internal pressure of

the artificial muscles in the hand was increased from 0.4 to 1.3 MPa. We assumed that the object could be gripped if the bent finger boosted up the object, and we performed gripping using the smallest applied pressure capable of gripping the object. With an applied pressure of 1.3 MPa, we confirmed that it is possible to grip a 500 kg object. We also performed similar grip tests using the 200 mm square and 165 mm cylindrical objects. The verification results of these gripping operations are shown in Fig. 19.

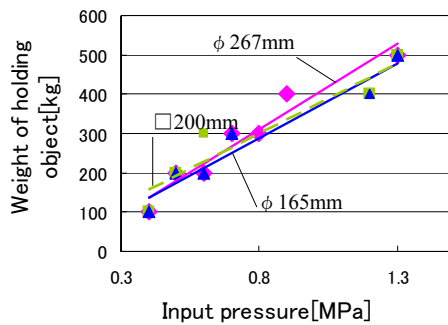


Fig. 19: The result of the holding test with 3 types of the obstacles

## VI. CONCLUSION

In this study, we used our high output water hydraulic artificial muscle to grip diverse objects by adapting the flexibility of the artificial muscles, and we developed a power hand capable of exerting large grip forces. The hand was made with 3 fingers, and we verified its ability to grip long massive objects. We also designed and built water hydraulic units to drive the hand, and we built a control device to control them. We performed mass gripping tests and confirmed that this hand is capable of gripping masses of up to 500 kg when the internal pressure in the artificial muscles is 1.3 MPa. We also verified the shape adaptation performance using gripping objects with three different shapes. The artificial muscles are also capable of gripping stably with higher applied pressures.

## REFERENCES

- [1] Mayuko Mori, Koichi Suzumori, Junichi Tanaka, Takefumi Kanda, "Development of Rescue Robot using Ultra High Pressure Hydraulic Small Actuators and Field Tests for Verification of their Possibilities," in *Journal of the Robotics Society of Japan*, Vol.25 No.5, 2007, pp.111-119.
- [2] Mayuko Mori, Koichi Suzumori, Shuichi Wakimoto, Masayuki Takahashi, Takashi Hosoya, Syukushi, "High Hydraulic McKibben type Muscle with Ultra-High-Strength PBO Cord Sleeve," in *The Proceedings on Spring Conference of Japan Fluid Power System Society*, 2008, pp. 17-19.
- [3] Mayuko Mori, Koichi Suzumori, Shuichi Wakimoto, Masayuki Takahashi, Takashi Hosoya, Syukushi, "High Hydraulic McKibben type Muscle with Ultra-High-Strength PBO Cord Sleeve," in *Journal of the Robotics Society of Japan*, 2008, 2P1A07.
- [4] Mayuko Mori, Harunori Shiosaki, Koichi Suzumori, Shuichi Wakimoto, Masayuki Takahashi, Takashi Hosoya, Emi Takematu,

- "Development of High Force Hydraulic McKibben type Artificial Muscle," in *The 27<sup>th</sup> Annual Conference of the Robotics Society of Japan*, to be published.
- [5] Mayuko Mori, Koichi Suzumori, Masayuki Takahashi, Takashi Hosoya, "Very High Force Hydraulic McKibben Artificial Muscle with PBO Cord Sleeve," in *Advanced Robotics(RSJ)*, to be published.
- [6] T.Kitagawa et al., "Structural Study on PBO Fiber," in *14th Annual Meeting*, Polymer Processing Society, 1998, pp. 723.
- [7] Michael Hannan, Ian Walker, "Vision Based Shape Estimation for Continuum Robots," in *2003 IEEE International Conference on Robotics & Automation*, 2003, pp. 3449-3454.
- [8] Bryan A. Jones, Ian D. Walker, "Limiting-case Analysis of Continuum Trunk Kinematics," in *2007 IEEE International Conference on Robotics and Automation*, 2007, pp. 1363-1368.
- [9] Koichi Suzumori, Shoichi Ikura, Hisohisa Tanaka, "Applying A Flexible Microactuator to Robotic Mechanisms," in *IEEE Control System*, Vol.12 No.1, 1992, pp.21-27.
- [10] Yhoichi Takamoto, "For useful robot. A track of the challenge to establish a company for development of robot," in *Journal of the Japan Society of Mechanical Engineers*, Vol.108 No.1036, 2005, pp.156-157.
- [11] 6th Fire District HQ TOKYO Fire Department HP, Available: <http://www.tfd.metro.tokyo.jp/hp-dai6honbu/6hr/kidoutokkatai.htm>
- [12] Mayuko Mori, Junichi Tanaka, Koichi Suzumori, Takefumi Kanda, "A Mobile Cutter Robot for Rescue Operations," in *SICE Annual Conference*, 2005, pp. 361-363.
- [13] Schulte, H. F., "The Characteristics of the McKibben Artificial Muscle," in *The Application of External Power in Prosthetics and Orthotics*, 1961, pp. 94-115.
- [14] Mayuko Mori, Koichi Suzumori, Masayuki Takahashi, Takashi Hosoya, "Very High Force Hydraulic McKibben Artificial Muscle with PBO Cord Sleeve," *Advanced Robotics(RSJ)*, Vol. 24, No. 1-2 (be published in 2010.1)
- [15] K.Kuribayashi, "Criteris for Evaluation of New Robot Actuators as Energy Converters," in *Journal of the Robotics Society of Japan*, 1989, Vol.7 No.5, pp. 35-45.
- [16] Horiuchi Machinery co.,Ltd, *Guidance of Hydraulic Cylinder for Professionals 2006 catalogue* in Japanese, 2006, pp.224.
- [17] Corp.CKD, *Union catalogue of air cylinders 1*, catalogue in Japanese, pp. 281.
- [18] Corp.NSK, catalogue in Japanese, catalogue No.CAT.NO.3157, B41,2001.
- [19] © 2005 Festo AG & Co. KG, *Catalogue of Rubber Muscle MAS series internal diameter φ10,20,40*, 2005, pp.12-14.
- [20] TACMINA Corporation, Magnet pump MG series, Instruction manual, 2005 in Japanese.
- [21] KYOWA Ltd., KYOWA TESTER, Instruction manual, KY-20A/KY-40A, 2007